Electronic structure of $Y_{2-x}Ca_xBaNiO_5$ from photoemission and inverse photoemission

K. Maiti and D. D. Sarma*
Solid State and Structural Chemistry Unit, Indian Institute of Science, Bangalore 560 012, India
(Received 9 January 1998)

We investigate the electronic structure of a one-dimensional spin-1 system, Y_2BaNiO_5, and hole-doped $Y_{2-x}Ca_xBaNiO_5$ for $x=0.2$ and 0.4, employing photoemission and inverse photoemission spectroscopies. Y_2BaNiO_5 has a charge excitation gap of about 2.3 eV. Hole doping via Ca substitution in this system introduces new localized states within this gap. The existence of a finite gap ($\sim$0.6 eV), even in doped compounds with a variable-range-hopping transport, indicates the importance of correlation effects and disorder in determining the electronic structure in this system. [S0163-1829(98)01739-1]

I. INTRODUCTION

Low-dimensional systems have attracted considerable attention in recent years, arising from their interesting physical properties such as transport,[1] magnetism,[2,3] and spin dynamics.[4–9] Such systems, particularly one-dimensional ones, provide an ideal testing ground for theoretical models, since exact analytical solutions can often be obtained at this limit. For example, it has been shown that one-dimensional spin chains with $S=1$ have a gap in the spin excitation spectra, whereas spin chains with $S=\frac{1}{2}$ have continuous excitations.[10] Systems with integer spin chains, exhibiting a gapped spin excitation spectrum, are known as *Haldane systems*, and their ground states as *Haldane states*. There have been extensive investigations using various experimental probes on several such systems with spin-1 chains[2–4] and spin-$\frac{1}{2}$ chains.[11–19] Electronic excitation spectra of this interesting class of compounds with integral spin chains, however, have not been investigated in detail.

Among all one-dimensional spin-1 systems, Y_2BaNiO_5 has been investigated most extensively due to its simple structure. Moreover, it is possible to sever the chains easily by substitution of trivalent Y with divalent Ca (Ref. 20). The structure of Y_2BaNiO_5 is orthorhombic with space group *Immm* (Refs. 20 and 21). The NiO_6 octahedra form a chainlike structure by sharing corners with a shorter bond length ($\sim$1.88 Å) along the chain direction (*z* direction) compared to the four equivalent bond lengths ($\sim$2.18 Å) perpendicular to the chain direction (*xy* plane). An absence of Ni-O-Ni interaction between the neighboring chains makes the electronic structure of this system an essentially one-dimensional one. This is further evidenced by the fact that though the antiferromagnetic interaction along the chain is strong, three-dimensional magnetic ordering has not been observed in this system down to 1.5 K (Ref. 22). Neutron-diffraction measurements show negligible inter-chain interaction ($\leqslant$0.05% of the intrachain interaction) in this system.[23] Y_2BaNiO_5 has a spin-liquid ground state with a gap ($\sim$10 meV) in the spin excitation spectrum.[1,4,23] Various theoretical approaches show the ground state to be a valence bond solid (VBS) state. Within this description, each $S=1$ spin is comprised of two $S=\frac{1}{2}$ entities with intersite neighbors bound into a singlet state.[8,9] However, the temperature dependence of the specific-heat measurements[24] at low temperatures could be explained by the existence of only spin-1 entities arranged antiferromagnetically, instead of the arrangement suggested in the VBS state. Activated behavior has been observed in this system in the transport properties with a transport gap of about 600 meV, which is much smaller than the charge gap of about 2 eV, as reported by DiTusa *et al.*[1] Neutron-diffraction studies show that while small ($\sim$4%) Zn substitution gives similar spin excitation spectrum, providing evidence for the unaltered Haldane phase in the smaller segments of the chains, hole doping by the substitution of divalent Ca in place of trivalent Y introduces spin excitation features within the Haldane gap. X-ray-absorption studies also show the existence of new charge states within the charge excitation gap, which have been characterized to be of O $2p_z$ character. In the present paper, we investigate the electronic structure of $Y_{2-x}Ca_xBaNiO_5$ for $x=0.0$, 0.2 and 0.4 by means of x-ray photoemission (XP), ultraviolet-photoemission (UP), and bremsstrahlung isochromat (BI) spectroscopic techniques in conjunction with band-structure calculations. The present results provide a detailed description of the electronic structure of the parent compound as well as the changes in the electronic structure on doping hole states into the system. It appears that both strong interaction effects and disorder play important roles in determining the evolution of the electronic structure in these compounds.

II. EXPERIMENT

$Y_{2-x}Ca_xBaNiO_5$ for $x=0.0$, 0.2, and 0.4 were prepared following the sol-gel route starting with stoichiometric amounts of predried Y_2O_3, $BaCO_3$, $CaCO_3$, and NiC_2O_4, $2H_2O$. The ingredients were dissolved in HNO_3 (least amount), and added to the solution of diluted citric acid with continuous stirring, where the amount of citric acid was more than the equivalent amount needed to convert the metal ions into corresponding citrates. This was followed by the addition of ethylene glycol to the solution in order to fix the *p*H for the maximum reaction, and stirred continuously to form a gel with uniform distribution of the metal ions. The obtained gel was dried by heating at low temperature followed by successive heatings at 350, 450, 600, 800, 900, 1000, and 1100 °C for 15 h each with in between grindings, and finally at 1180 °C for 24 h. The sample was cooled down from the final temperature to 300 °C at the rate of 3 °C/min to maintain the proper oxygen stoichiometry as described by Alonso *et al.*[20] X-ray-diffraction patterns estab-

lish each composition to be in single phase. All the samples were characterized by transport and magnetic measurements and the present results compare well with those in the published literature.[1–3,25] Photoemission and inverse photoemission spectroscopic measurements were carried out in a combined electron spectrometer equipped with Mg $K\alpha$ source, He discharge lamp and electron gun. The resolutions associated with the XP, UP, and BI spectroscopic measurements were 0.8 eV, 90 meV, and 0.8 eV, respectively. BI spectroscopic measurements were carried out by detecting the photons at a fixed energy of 1486.6 eV, and varying the incident electron energies. The sample surface was cleaned in each case by periodical *in situ* scraping with an alumina file and monitored by the oxygen 1*s* feature and the integrated carbon 1*s* intensities. The reproducibility of the spectral features was confirmed in each case.

A spin-polarized scalar relativistic linearized muffin-tin orbital calculation has been performed within the atomic-sphere approximation (LMTO-ASA) for Y_2BaNiO_5 with 36 atoms per unit cell (four formula units). The lattice parameters are $a=11.3311$ Å, $b=5.7604$ Å, and $c=3.7589$ Å. Here the chain axis is along the *c* direction. The sphere radii used in this calculation are 1.8432, 2.0673, 1.4811, and 0.9945 Å for Y, Ba, Ni, and O, respectively. No empty sphere was required to satisfy the volume filling criterion used in the atomic-sphere approximation. In this calculation, convergence was obtained self-consistently using *s*, *p*, and *d* basis states at each atomic sphere with 64 *k* points in the irreducible part of the Brillouin zone. The energies E_ν^l for each angular momentum partial wave were chosen to be the center of gravity of the occupied part of the corresponding partial density of states (PDOS). The calculation was carried out for the antiferromagnetic order along the chain direction. Since the magnetic measurements show negligible interaction in between the chains with no three-dimensional ordering down to 1.5 K, we have not considered various spin arrangements perpendicular to the chain direction. In order to obtain theoretical spectra to compare with experimental XP spectra, it is necessary to include the effects of matrix elements.[26] Thus, theoretical spectra based on the band-structure calculation were constructed by multiplying the various PDOS with corresponding matrix elements and convoluting with a Lorentzian with energy-dependent full width at half maximum representing the lifetime broadening.[27–29] The resolution broadening has been introduced by convoluting with an appropriate Gaussian describing the resolution function. In order to align various spectral features, the calculated spectral functions are shifted by 1 eV toward higher binding energy. This is usually necessary for the strongly correlated systems due to the underestimation of band gaps in these calculations.[30]

III. RESULTS AND DISCUSSIONS

We show the valence-band photoemission spectra of Y_2BaNiO_5 in Fig. 1 for the incident photon energies 21.2 eV (He I), 40.8 eV (He II) and 1253.6 eV (XPS). The spectra are normalized at the most intense peak around 5-eV binding energy. There are three discernible features *A*, *B*, and *C* in the He I spectrum at about 2.4-, 3.5-, and 5.0-eV binding energies, respectively. With the increase in the incident photon energy to 40.8 eV in the He II photoemission measurement, the intensity of the feature *B* decreases considerably while that of the feature *A* increases compared to the 5.0-eV peak (feature *C*). The intensity of feature *A* is further enhanced in the XP spectrum recorded with much larger photon energy (1253.6 eV). It is well known[31] that photoemission cross sections for oxygen 2*p*-like states are larger relative to the transition-metal 3*d*-like states at low photon energies (21.2 eV), and the photoemission cross-section ratio between these two states monotonically decreases with increasing photon energy, favoring the transition metal 3*d* contribution to the spectra at higher energies. Thus the relative changes in the spectral intensities in Fig. 1, with the increase in photon energy, indicate that the spectral region in the vicinity of 2.4-eV spectral feature (*A*) is dominated by Ni 3*d* emission, while those near the 3.5- and 5.0-eV features have more oxygen 2*p* character. A pronounced reduction of the 3.5-eV feature compared to that at 5.0 eV indicates that the states near 3.5 eV is primarily formed by O 2*p*–O 2*p* interactions with a nonbonding character with respect to Ni 3*d*–O 2*p* interactions.

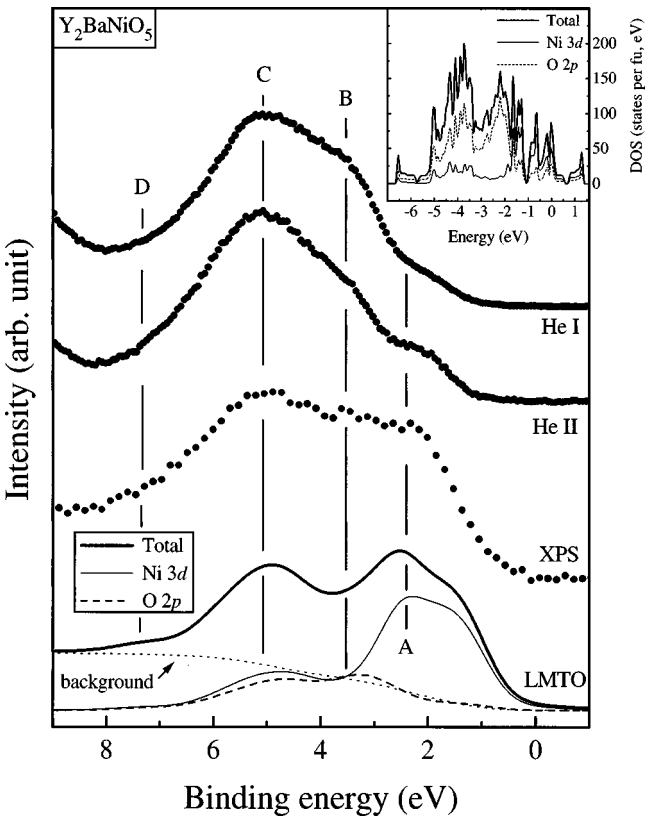

FIG. 1. He I, He II, and XP spectra of Y_2BaNiO_5. The spectral functions obtained from LMTO-ASA band-structure calculations are also shown in the figure. The thick solid line shows the total spectral function including an integral background. The thin solid line and the dashed line correspond to the spectral functions of Ni 3*d* and O 2*p* PDOS. The short dashed line represents the integral background. The inset shows the DOS obtained from spin-polarized LMTO-ASA calculation, with O 2*p* (dashed line) and Ni 3*d* (thin solid line) PDOS. fu is the formula unit.

In order to compare the experimental spectra with the band structure results, we compute the theoretical spectrum starting from PDOS of all the states obtained from LMTO-ASA band-structure calculations as explained earlier. We

have performed both spin-polarized and unpolarized calculations. In the case of the spin-polarized calculation, a magnetic structure with an antiferromagnetic arrangement of the Ni atoms along the chain was found to have lower energy than a nonmagnetic solution in conformity with experimental observations.[2,3] However, a metallic ground state, obtained in both the calculations, is in contrast to the insulating property. It is important to note here that a small amount of disorder in one-dimensional systems can lead to a localization of charge carriers, thereby giving rise to an insulating ground state. However, such effects will not produce a large charge excitation gap; in contrast, the corresponding gap in this system, as we show later in the text, is about 2.3 eV. Thus the insulating ground state observed here does not originate from the disorder effects. The large charge excitation gap obtained in this compound, and the failure of the band structure to describe this gap, thus arises from the presence of strong electron correlations in the system. Such band-structure calculations are, indeed, known to underestimate correlation effects. The calculated spectral features, corrected for the matrix element effects for x-ray-photoemission measurements and including the resolution broadening as well as energy-dependent lifetime broadening are plotted in Fig. 1 with the corresponding PDOS, and Ni $3d$ and O $2p$ PDOS shown in the inset. In order to compare the calculation with the experiment, an integral background (shown as a short dashed line) has been added to the calculated total spectrum (the thick solid line). The thin solid line and the dashed line correspond to the PDOS of Ni $3d$ states and the oxygen $2p$ states, respectively. It is clear from the figure that the lower-binding-energy region (<3 eV) is dominated by the Ni $3d$-like states, and the region with higher binding energy (>3 eV) is nearly equally contributed by the Ni $3d$- and O $2p$-like states. However, the PDOS shown in the inset clearly shows the dominance of O $2p$ PDOS in the higher-energy region; thus, the similar calculated spectral intensities for Ni $3d$ and O $2p$ states arise from a larger photoemission cross section for the Ni $3d$ states at this high photon energy. Noting the substantial admixture of Ni $3d$ states in the vicinity of 5-eV binding energy, this DOS region, responsible for the spectral feature *C*, is assigned to the O $2p-$Ni $3d$ bonding states with a dominant oxygen $2p$ character. Similarly, the feature (*A*) around 2.4 eV is attributed to the corresponding antibonding states, where the dominant contribution comes from the Ni $3d$ states. The spectral feature at 3.5 eV binding energy (*B*), which is more pronounced in the He I spectrum, is not clearly discernible in the calculated total spectrum, primarily due to an underestimation of the oxygen $2p$ photoemission cross section.[30] However, this feature, dominated by the oxygen $2p$ states, can also be observed at the same energy both in the DOS and PDOS shown in the inset as well as in the calculated oxygen $2p$ contribution (long dashed line). The inset shows that there is little Ni $3d$ contribution in the vicinity of this energy region. This confirms that the states in this energy region arise primarily due to oxygen $2p$-$2p$ interactions with a nonbonding character with respect to Ni $3d-$O $2p$ interactions. There is a weak, broad feature at about 7.5 eV in the calculated spectrum; this feature is also discernible in the experimental XP spectrum (marked *D*). It originates from the corresponding DOS features between about 6 and 7 eV (see inset), and arises from oxygens along the chains.[32]

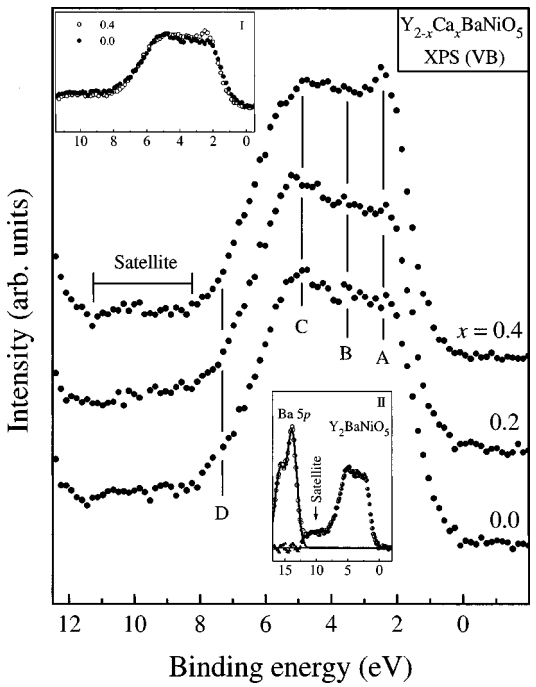

FIG. 2. XP spectra of $Y_{2-x}Ca_xBaNiO_5$ for $x=0.0$, 0.2, and 0.4 showing the changes due to doping. In inset I we overlap the spectra corresponding to $x=0.0$ (solid circles) and 0.4 (open circles). In inset II we illustrate the presence of a satellite feature in the valence-band spectrum of Y_2BaNiO_5 (open circles) by subtracting the Ba $5p$ contributions (solid line) after appropriate background subtraction. The subtracted spectrum is shown by solid triangles.

The calculated spectrum within the local-density approximation appears to provide a reasonable description of the higher-binding-energy features between about 3 and 8 eV in terms of peak shape, width, and position. This is not surprising, since these features are primarily dominated by oxygen $2p$ states, which are not very much influenced by correlation effects. On the other hand, it is clear that the Ni $3d$-related spectral features appearing at lower binding energies are considerably distorted in the experimental spectrum compared to the calculated ones, evidencing a strong influence of correlation effects in this compound.

The substitution of one divalent Ca at the place of trivalent Y enhances the effective valency of Ni by 1 and, thus, one hole is doped in the system. In order to investigate the effect of such doped holes on the electronic structure, we plot the XP valence-band spectra for $x=0.0$, 0.2, and 0.4 in Fig. 2. All the spectra have been normalized at the peak around the 20.8-eV binding energy contributed by O $2s$ and Ba $5s$ states (not shown in the figure), since the intensity of these signals is not expected to change with Ca doping at the Y site. All the spectra exhibit low-intensity spectral features between 8- and 11-eV binding energies. The tail of the Ba $5p$-related features at higher energies overlaps strongly the satellite feature, as shown in inset II of Fig. 2 for Y_2BaNiO_5. Subtracting Ba $5p$ contributions (shown by a solid line in inset II) from the total spectrum (open circles), and thus obtaining the difference spectrum (solid triangles), it becomes possible to estimate the relative intensity of the satellite as illustrated by the significant intensity beyond 8-eV binding

energy in inset II. The calculated spectrum based on *ab initio* band-structure results shown in Fig. 1 does not have any intensity beyond 8 eV; this suggests that the satellite features arise from correlation effects, not included in such effectively independent-particle approaches. The features arising from primarily oxygen $2p$ PDOS in the vicinity of spectral signatures *B* and *C* are found to be nearly unchanged on doping, as more clearly illustrated in inset I by overlapping the spectra of $x=0.0$ and 0.4. Since this spectral feature arises primarily from the bonding $2p$ states of the oxygens on the basal plane perpendicular to the chain direction,[32] the insensitivity at this spectral region suggests that the hole doping does not significantly influence these states. This is in conformity with the results in Ref. 1 that the doped holes have primarily Ni $3d_{z^2}-O\ 2p_z$ characters. On the other hand, there is a slight narrowing and a consequent emergence of a sharper Ni $3d$-related spectral feature (A) at about 2.4 eV with increasing doping. Concomitantly, the intensity around 7–9-eV binding energy reduces (see inset I). Thus, the main effect of hole doping on the electronic structure in the occupied part appears to be a slight reduction in intensity at the band edges, manifested as a narrowing of the band. It is to be noted here that the doping of hole states in three-dimensional NiO by substituting Li at the place of Ni introduce an overall reduction in $3d$ band intensity without any significant change in the shape of the spectral features.[33] While calculations based on cluster or impurity models are likely to throw light on these effects, the model will necessarily have to include more than one Ni site in order to describe the nonintegral doping levels. Such calculations including the multiplet interactions at multiple impurity sites are beyond the scope of the present computational ability.

The doped holes, however, show pronounced changes in the unoccupied part of the electronic structure, as illustrated in Fig. 3. Here we plot the BI spectra corresponding to $x=0.0$, 0.2, and 0.4, normalizing them at the narrow Ba $4f$ peak position at about 14 eV above E_F, since the Ba content is fixed in all the compositions. For comparison, we overlap the spectrum corresponding to $x=0.0$ (shown by the open circles) on the spectra of $x=0.2$ and 0.4. The relatively broad feature *C* with the center of gravity around 8 eV above the Fermi level in the parent compound ($x=0.0$) is contributed by the Ba $5d$ and Y $4d$ states. The spectrum of Y_2BaNiO_5 shows a distinct shoulder at about 3.5 eV (marked *B*) above E_F. This feature is attributed to the spectral signature of the upper Hubbard band arising mainly from Ni $3d$ states. On substituting Ca for Y, there is a decrease in the intensity of feature *C*, associated with a decrease of Y $4d$ contribution to the spectrum. The most pronounced changes are, however, seen closer to the Fermi energy in the energy region of the upper Hubbard band. We find a progressive reduction in the intensity of the spectral feature *B* at about 3.5 eV, corresponding to the peak of the upper Hubbard band of the stoichiometric Y_2BaNiO_5 with doping. This is accompanied by the clear emergence of a spectral feature (*A*) closer to E_F peaking at about 1 eV, due to the doped hole states. The increase in intensity of these doped states is evidently more rapid than the reduction in the spectral weight of the upper Hubbard band. Such a spectral weight transfer has indeed been observed in the O *K*-edge x-ray absorption (XA) spectroscopy of this system.[1] In that study it was observed that

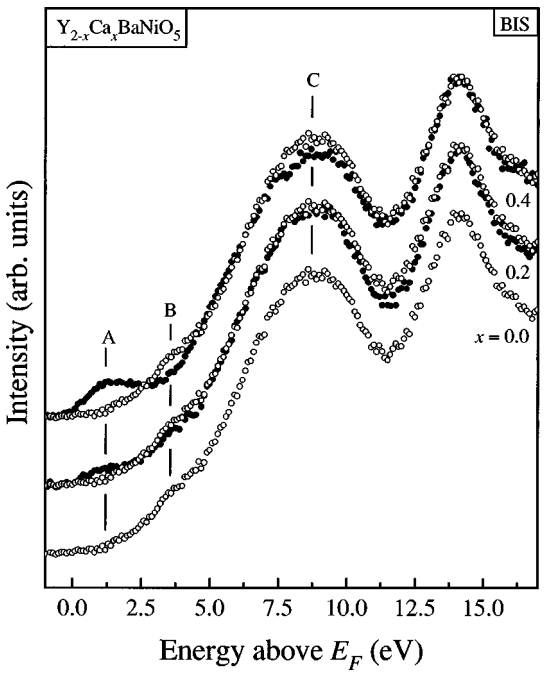

FIG. 3. BI spectra of $Y_{2-x}Ca_xBaNiO_5$ for $x=0.0$, 0.2, and 0.4. The spectrum corresponding to $x=0.0$ (open circles) is overlapped over the spectra corresponding to $x=0.2$ and 0.4 in order to indicate the changes in the spectra clearly.

the electric polarization vector along the chain direction exhibits a spectral weight transfer with negligible change along perpendicular polarizations. Thus, in conjunction with the XA results, the feature around 3.5 eV above the Fermi level (E_F) observed in Fig. 3 can be characterized to be arising from the upper Hubbard band (UHB) primarily with $3d_{z^2}$ (a_{1g}) symmetry. The feature corresponding to the upper Hubbard band with $3d_{x^2-y^2}$ (b_{1g}) symmetry observed in the XA study is expected to arise around 2.5 eV above E_F [the splitting of the e_g band arising from the distortion of the NiO_6 octahedra is about 0.91 eV (Ref. 1)], which is barely discernible in the figure possibly due to the resolution broadening and the consequent tailing of the higher-energy intense features near 8 eV. The spectral weight transfer as observed in the UHB (a_{1g}) in this system as a function of doping, was observed in the BI as well as XA spectra of other divalent nickelates, such as $Li_xNi_{1-x}O$ (Refs. 33,34) and $La_{2-x}Sr_xNiO_4$.[35–37] In all these cases the doped states are found to appear above the Fermi level (E_F) ($\sim$1 eV), extending down in energy toward E_F, but without contributing any intensity at E_F in accordance with the insulating phase in all these cases. It is interesting to note here that such anomalous spectral weight transfer has also been observed in divalent spin-$\frac{1}{2}$ cuprate systems,[38–40] and is believed to be driven by the strong electron-correlation effects.[41] Thus, while the spin dynamics of this spin-1 chain system, $Y_{2-x}Ca_xBaNiO_5$, exhibits substantially different physics compared to those observed in the case of half-integer spin chains, and the divalent nickelates and cuprates in higher dimensions, the charge dynamics is found to be essentially similar in all the cases.

In order to understand the evolution of the low-energy charge excitation spectra in these compounds, we investigate next the spectral features close to E_F combining the spectra

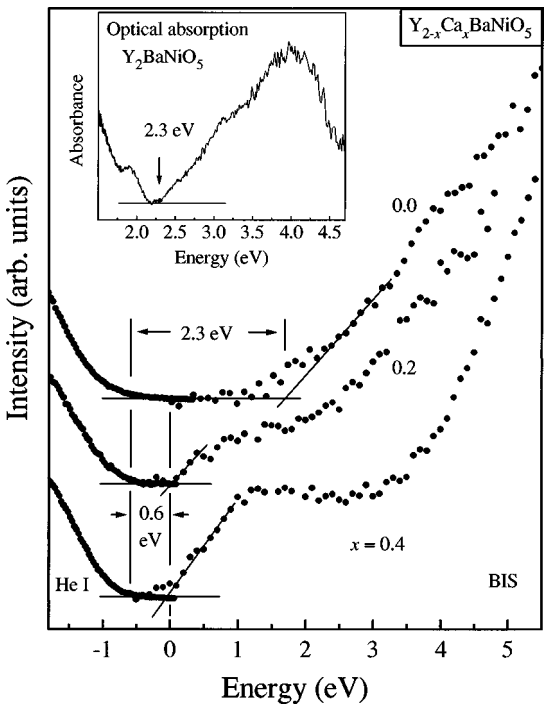

FIG. 4. He I and BI spectra of $Y_{2-x}Ca_xBaNiO_5$ ($x=0.0$, 0.2, and 0.4) with a common Fermi level in order to show the charge excitation gap. The inset shows the optical (UV-VIS) absorption spectrum of Y_2BaNiO_5 indicating a charge excitation gap of about 2.3 eV.

from the occupied and unoccupied parts. We combine the He I photoemission and BI spectra in Fig. 4 with a common Fermi energy to estimate the charge excitation gap in Y_2BaNiO_5. It is difficult to determine the band edges precisely from these experimental spectra, since the bands are broadened in the experimental spectra due to the presence of finite resolution. Thus, we adopt an approach which has been useful in the past in determining the band edges in $LaCrO_3$,[42] $LaMnO_3$,[43] and $LaFeO_3$,[44] by drawing tangents to the rapidly changing leading edges of the experimental spectrum as illustrated in the figure. This procedure estimates the band gap to be about 2.3 ± 0.3 eV in Y_2BaNiO_5. These results are further confirmed by the optical absorption spectrum obtained from diffused reflectance measurements for Y_2BaNiO_5 shown in the inset. It clearly shows the absorption edge around 2.3 eV, which agrees well with the gap estimated from the UP and BI spectra. The estimate of the intrinsic band gap obtained here is substantially larger than the activation energy (0.6 eV) observed in the resistivity measurements.[1] Thus it appears that the resistivity in the measured temperature range is dominated by contributions from impurity states inevitably present within the intrinsic band gaps of such transition-metal oxides arising from finite deviations from the ideal stoichiometry.

The narrow energy range of the He I and BI spectra for $x=0.2$ and 0.4 near E_F are shown in Fig. 4. It is evident from the spectra that there is no spectral intensity at E_F and spectral features exhibit clear signatures of gaps in the charge excitation spectra of the doped compounds. However, the spectral intensity in the BI spectra of the doped compounds appears considerably closer to E_F compared to the undoped compound, leading to a substantial decrease of the gap. This is clearly due to the formation of hole states arising from doping; these doped states form within the charge-transfer band gap of the parent compound, as is evident in the spectra shown in Fig. 4. We estimate the gap to be about 0.6 eV in both the doped compounds, as shown in the figure. This is close to the activation energy extracted from the resistivity measurements below room temperature on the parent compound. Thus it appears that the conductivity gap at lower temperatures is controlled by states doped within the charge-excitation gap of the ideally stoichiometric compound, due to the inevitable presence of nonstoichiometry and defects. The existence of a pronounced gap of about 0.6 eV in the doped compounds is in apparent contrast with the observation[1] of variable-range-hopping transport, suggesting a finite density of states at E_F. However, we note that the size of the gap is considerably larger than the thermal energy scale over which the resistivity measurements were carried out (<300 K). In such a situation, the low-temperature (<300 K) resistivity can be dominated by very low density of states, below the level of photoemission sensitivity, if such states are present in the vicinity of the Fermi energy. Besides the existence of such a low density of states across E_F influencing the low-temperature transport properties, the electronic structure of the doped systems is clearly dominated by the formation of the midgap doped hole states, in agreement with the results obtained in Ref. 45 based on the dynamical hole approach. However, the prediction of a finite ω precursor of Drude peaks in the optical conductivity comprising the hole states delocalized over a sizable, but finite, length scale, is in contrast to the observation of a large distinct gap (~0.6 eV) in the doped compounds. These observations suggest that a disorder-induced Anderson localization, or the electron-correlation effect, alone is not sufficient to explain the changes in the electronic structure of the doped compounds. Strong correlation effects which drive the gap formation will have to be taken into account simultaneously with the disorder effects. In this context, it is interesting to note that a recent treatment of simultaneous presence of disorder and electron-electron interactions has suggested[46] characteristic signatures of disorder in terms of localized states across E_F, and an overall gaplike structure driven by correlation.

In conclusion, we have investigated the electronic structure of Y_2BaNiO_5 and the effect of hole doping in this system via substitution of Y^{3+} by Ca^{2+}. Y_2BaNiO_5 is a correlation-driven insulator with a charge excitation gap of about 2.3 eV. Band-structure calculations based on the local-density approximation cannot describe the insulating ground state. The doping reduces the overall bandwidth slightly in the occupied part of the electronic structure. More pronounced changes are observed in the spectra corresponding to the unoccupied part of the electronic structure. Doped hole states are formed in the charge gap of the parent compound; the intensity of this feature grows systematically with anomalous spectral weight transfer from the Hubbard bands, similar to that observed in the higher-dimensional divalent nickelates (NiO and La_2NiO_4). The doped compounds also exhibit a distinct gap of about 0.6 eV, though the transport measurements exhibit a variable range hopping instead of an activated behavior. The presence of this finite-gap-like structure for all the compositions, along with the evidence of a low, but finite, density of states from resistivity measure-

ments, suggests an interplay of disorder and correlation effects to be important in determining the electronic structure of these compounds.

ACKNOWLEDGMENTS

The authors thank Professor C.N.R. Rao for continued support, the Department of Science and Technology, Government of India, for financial assistance, and the Supercomputer Education and Research Center for providing computational facilities. D. D. S. thanks Dr. M. Methfessel, Dr. A. T. Paxton, and Dr. M. van Schiljgaarde for making the band-structure program available and Dr. S. Krishnamurthy for initial help in setting up the band-structure program. K. M. thanks the Council of Scientific and Industrial Research, Government of India, for financial assistance.

*Also at Jawaharlal Nehru Center for Advanced Scientific Research, Bangalore, India.
Electronic address: sarma@sscu.iisc.ernet.in

[1] J. F. DiTusa, S.-W. Cheong, J.-H. Park, G. Aeppli, C. Broholm, and C. T. Chen, Phys. Rev. Lett. **73**, 1857 (1994).
[2] S. Ma, C. Broholm, D. H. Reich, B. J. Sternlieb, and R. W. Erwin, Phys. Rev. Lett. **69**, 3571 (1992).
[3] W. J. L. Buyers, R. M. Morra, R. L. Armstrong, M. J. Hogan, P. Gerlach, and K. Hirakawa, Phys. Rev. Lett. **56**, 371 (1986).
[4] J. Darriet and L. P. Regnault, Solid State Commun. **86**, 409 (1993).
[5] Z.-Y. Lu, Z.-B. Su, and L. Yu, Phys. Rev. Lett. **74**, 4297 (1995).
[6] M. Hagiwara, K. Katsumata, I. Affleck, B. I. Halperin, and J. P. Renard, Phys. Rev. Lett. **65**, 3181 (1990).
[7] J. Deisz, M. Jarrel, and D.-L. Cox, Phys. Rev. B **42**, 4869 (1990).
[8] I. Affleck, T. Kennedy, E. H. Lieb, and H. Tasaki, Phys. Rev. Lett. **59**, 799 (1987).
[9] P. P. Mitra, B. I. Halperin, and I. Affleck, Phys. Rev. B **45**, 5299 (1992).
[10] F. D. M. Haldane, Phys. Lett. **93A**, 464 (1983); Phys. Rev. Lett. **50**, 1153 (1983).
[11] K. Maiti, D. D. Sarma, T. Mizokawa, and A. Fujimori, Phys. Rev. B **57**, 1572 (1998).
[12] K. Maiti, D. D. Sarma, T. Mizokawa, and A. Fujimori, Europhys. Lett. **37**, 359 (1997).
[13] H. Suzuura, H. Yasuhara, A. Furusaki, N. Nagaosa, and Y. Tokura, Phys. Rev. Lett. **76**, 2579 (1996).
[14] N. Motoyama, H. Eisaki, and S. Uchida, Phys. Rev. Lett. **76**, 3212 (1996).
[15] S. Kondoh, K. Fukuda, and M. Sato, Solid State Commun. **65**, 1163 (1988).
[16] M. Knupfer, R. Neudert, M. Kielwein, S. Haffner, M. S. Golden, J. Fink, C. Kim, Z.-X. Shen, M. Merz, N. Nücker, S. Schuppler, N. Motoyama, H. Eisaki, S. Uchida, Z. Hu, M. Domke, and G. Kaindl, Phys. Rev. B **55**, R7291 (1997).
[17] K. Ishida, Y. Kitaoka, Y. Tokunaga, S. Matsumoto, K. Asayama, M. Azuma, Z. Hiroi, and M. Takano, Phys. Rev. B **53**, 2827 (1996).
[18] O. V. Misochko, S. Tajima, C. Urano, H. Eisaki, and S. Uchida, Phys. Rev. B **53**, 14 733 (1996).
[19] C. Kim, A. Y. Matsuura, Z.-X. Shen, N. Motoyama, H. Eisaki, S. Uchida, T. Tohyama, and S. Maekawa, Phys. Rev. Lett. **77**, 4054 (1996).
[20] J. A. Alonso, I. Rasines, J. Rodríguez-Carvajal, and J. B. Torrance, J. Solid State Chem. **109**, 231 (1994).
[21] J. Amador, E. Gutiérrez-Puebla, M. A. Monge, I. Rasines, C. Ruíz-Valero, F. Fernández, R. Sáez-Puche, and J. A. Campá, Phys. Rev. B **42**, 7918 (1990).
[22] J. A. Alonso, J. Amador, J. L. Martínez, I. Rasines, J. Rodríguez-Carvajol, and R. Séz-Puche, Solid State Commun. **76**, 467 (1990).
[23] G. Xu, J. F. DiTusa, T. Ito, K. Oka, H. Takagi, C. Broholm, and G. Aeppli, Phys. Rev. B **54**, R6827 (1996).
[24] A. P. Ramirez, S.-W. Cheong, and M. L. Kaplan, Phys. Rev. Lett. **72**, 3108 (1994).
[25] K. Maiti, N. Y. Vasanthacharya, and D. D. Sarma (unpublished).
[26] H. Winter, P. J. Durham, and G. M. Stocks, J. Phys. F **14**, 1047 (1984).
[27] D. D. Sarma, F. U. Hillebrecht, W. Speier, N. Mårtensson, and D. D. Koelling, Phys. Rev. Lett. **57**, 2215 (1986).
[28] W. Speier, E. V. Leuken, J. C. Fuggle, D. D. Sarma, L. Kumar, B. Dauth, and K. H. J. Buschow, Phys. Rev. B **39**, 6008 (1989).
[29] A. Fujimori and F. Minami, Phys. Rev. B **30**, 957 (1984).
[30] D. D. Sarma, N. Shanthi, S. R. Barman, N. Hamada, H. Sawada, and K. Terakura, Phys. Rev. Lett. **75**, 1126 (1995).
[31] J. J. Yeh and I. Lindau, At. Data Nucl. Data Tables **32**, 1 (1985).
[32] L. F. Mattheiss, Phys. Rev. B **48**, 4352 (1993).
[33] J. van Elp, H. Eskes, P. Kuiper, and G. A. Sawatzky, Phys. Rev. B **45**, 1612 (1992).
[34] P. Kuiper, G. Kruizinga, J. Ghijsen, G. A. Sawatzky, and H. Verweij, Phys. Rev. Lett. **62**, 221 (1989).
[35] H. Eisaki, S. Uchida, T. Mizokawa, H. Namatame, A. Fujimori, J. van Elp, P. Kuiper, G. A. Sawatzky, S. Hosoya, and H. Katayama-Yoshida, Phys. Rev. B **45**, 12 513 (1992).
[36] E. Pellegrin, J. Zaanen, H.-J. Lin, G. Meigs, C. T. Chen, G. H. Ho, H. Eisaki, and S. Uchida, Phys. Rev. B **53**, 10 667 (1996).
[37] P. Kuiper, J. van Elp, G. A. Sawatzky, A. Fujimori, S. Hosoya, and D. M. de Leeuw, Phys. Rev. B **44**, 4570 (1991).
[38] C. T. Chen, F. Sette, Y. Ma, M. S. Hybertsen, E. B. Stechel, W. M. C. Foulkes, M. Schluter, S.-W. Cheong, A. S. Cooper, L. W. Rupp, Jr., B. Batlogg, Y. L. Soo, Z. H. Ming, A. Krol, and Y. H. Kao, Phys. Rev. Lett. **66**, 104 (1991).
[39] S. L. Cooper, G. A. Thomas, J. Orenstein, D. H. Rapkine, A. J. Millis, S.-W. Cheong, A. S. Cooper, and Z. Fisk, Phys. Rev. B **41**, 11 605 (1990).
[40] S. Tajima, S. Tanaka, T. Ido, and S. Uchida, in *Proceedings of the Second International Symposium on Superconductivity, Tsukuba, 1989*, edited by T. Ishiguro and K. Kajimura (Springer-Verlag, Berlin, 1990); K. Kitazawa and S. Tajima, in *Some Aspects of Superconductivity*, edited by L. C. Gupta (Nova, New York, 1990).
[41] H. Eskes, M. B. J. Meinders, and G. A. Sawatzky, Phys. Rev. Lett. **67**, 1035 (1991).
[42] K. Maiti and D. D. Sarma, Phys. Rev. B **54**, 7816 (1996).
[43] A. Chainani, M. Mathew, and D. D. Sarma, Phys. Rev. B **47**, 15 397 (1993).
[44] A. Chainani, M. Mathew, and D. D. Sarma, Phys. Rev. B **48**, 14 818 (1993).
[45] E. Dagotto, J. Riera, A. Sandvik, and A. Moreo, Phys. Rev. Lett. **76**, 1731 (1996).
[46] V. Dobrosavljević and G. Kotliar, Phys. Rev. Lett. **78**, 3943 (1997), and references therein.